

# Casimir–Polder interaction of neutrons with metal or dielectric surfaces

Valentin Gebhart,<sup>1</sup> Juliane Klatt,<sup>1</sup> and Stefan Yoshi Buhmann<sup>1,2</sup>

<sup>1</sup>*Physikalisches Institut, Albert-Ludwigs-Universität Freiburg,  
Hermann-Herder-Str. 3, 79104 Freiburg, Germany*

<sup>2</sup>*Freiburg Institute for Advanced Studies, Albert-Ludwigs-Universität Freiburg, Albertstr. 19, 79104 Freiburg, Germany*  
(Dated: April 28, 2018)

We predict a repulsive Casimir–Polder-type dispersion interaction between a single neutron and a metal or dielectric surface. Our model scenario assumes a single neutron subject to an external magnetic field. Due to its intrinsic magnetic moment, the neutron then forms a magnetisable two-level system which can exchange virtual photons with a nearby surface. The resulting dispersion interaction between a purely magnetic object (neutron) and a purely electric one (surface) is found to be repulsive. Its magnitude is considerably smaller than the standard atom–surface Casimir–Polder force due to the magnetic nature of the interaction and the smallness of the electron-to-neutron mass ratio. Nevertheless, we show that it can be comparable to the gravitational potential of the same surface.

PACS numbers: 12.20.–m, 42.50.Ct, 42.50.Nn, 03.75.Dg

As originally conceived by Casimir, the attractive force between two perfectly conducting parallel plates is a consequence of the quantum fluctuations of the electromagnetic field which persist even when the latter is in its vacuum state of zero temperature [1]. The plates, which are merely loci of boundary conditions supporting standing-wave modes of the electromagnetic field in this picture, are assigned a much more active role in Lifshitz’ theory for two dielectric plates [2]: Here, the fluctuating polarisations within the dielectric media ultimately generate the force. It is hence apparent that dispersion forces may much more generally arise as effective electromagnetic forces between any polarisable objects. They may be attributed to quantum zero-point fluctuations of the objects’ polarisation and of the electromagnetic field [3]. In particular, the term Casimir–Polder force is commonly used to refer to the dispersion interaction between a microscopic object such as an atom or a molecule and a macroscopic body [4].

Shortly after Casimir’s seminal work, it was found by Boyer that the force between a perfectly conducting plate and an infinitely permeable one is repulsive [5]. Mathematically, this is due to the different boundary conditions that electric vs magnetic mirrors place on the electromagnetic field [6]: the force depends on the product of the reflection coefficients of the two plates and is hence attractive for two electric or two magnetic mirrors and repulsive for two mirrors of different type. Repulsive dispersion forces have been predicted for a variety of scenarios involving a polarisable and a magnetisable object [7–10], including the Casimir–Polder force between an atom and a plate [11–14]. While the attractive Casimir–Polder force between a polarisable atom and a perfect electric mirror is a straightforward consequence of the attractive alignment of the fluctuating atomic dipole moment and its image [15], an understanding of the repulsion for mixed electric–magnetic object combinations re-

quires dynamical considerations. As explicitly shown for the case of two atoms, an oscillating electric dipole generates a magnetic field which orients a nearby magnetic dipole such that a repulsive force emerges [16, 17].

The study of repulsive dispersion forces is motivated by the hope that these could help overcome the problem of stiction in nanotechnology [18]. Theoretical studies have unearthed three mechanisms by which repulsion can be achieved, two of which have been verified experimentally: (i) Two bodies immersed in a liquid repel each other when one of them is more optically thin and the other more optically thick than the medium [19], the effect being analogous to an air bubble in water experiencing ‘repulsive gravity’. (ii) Non-equilibrium systems such as non-uniform temperatures [20] or excited atoms in a low-temperature environment [21] may experience repulsion, which is analogous to the force that an oscillating dipole exerts on a second, out-of-phase dipole of lower eigenfrequency. (iii) The mentioned repulsion due to magnetic properties has proven elusive so far, because for materials existing in nature it is typically overwhelmed by the ever-present attractive electric–electric force [10]. Attempts to overcome this problem via artificial metamaterials [9, 22, 23] have been demonstrated to fail due to an Earnshaw no-go theorem [24].

Here, we propose a system that is free from such constraints, because one of the interacting partners—a neutron—is purely magnetic. While electrically neutral and non-polar, the neutron does exhibit a magnetic moment which may interact with the quantum electrodynamic field. As we will argue, the neutron with its spin eigenstates can be viewed as a magnetisable two-level system which will experience a repulsive force of Casimir–Polder type when interacting with a metal or dielectric wall.

Evidence for interactions of neutrons with walls has been found within the context of neutron interferometry.

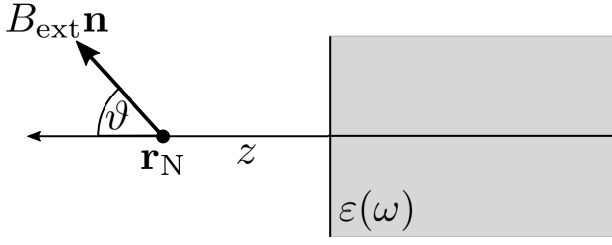


FIG. 1: Setup: Neutron in front of an infinite metal or dielectric plate. To lift the degeneracy of the two neutron spin states, an external magnetic field is applied in a direction  $\mathbf{n}(\vartheta)$  which is at an angle  $\vartheta$  with respect to the surface normal.

In particular, by introducing a stack of narrow slits into one arm of such an interferometer, a confinement-induced phase shift has been found [25]. Here, the plates forming the slits provide rigid boundary conditions for the neutron wave function. This is in contrast to our proposed long-range Casimir–Polder interaction which should be felt by the entire neutron wave function within such slits.

The article is organised as follows: we begin by describing the proposed setup of a neutron in front of a metal or dielectric surface and introduce the basic formalism of macroscopic quantum electrodynamics used to describe the surface-assisted magnetic field. We then derive the Casimir–Polder force on the neutron using second-order perturbation theory. Finally, we quantify the resulting neutron–plate interaction for different substrate materials and compare it to gravitational potentials.

*Setup and basic equations.* As illustrated in Fig. 1, we consider a single neutron at position  $\mathbf{r}_N$ , which is at a distance  $z$  from a homogeneous metal or dielectric plate of electric permittivity  $\varepsilon(\omega)$  which is infinitely thick and infinitely extended in the lateral dimensions (semi-infinite half space).

In order to obtain the Casimir–Polder potential of the neutron, we separate the Hamiltonian into the free Hamiltonians of the neutron and the medium-assisted electromagnetic field on one side and the interaction Hamiltonian on the other. We treat the latter as a perturbation. The free field Hamiltonian is given by [26]

$$\hat{H}_F = \int d^3\mathbf{r} \int_0^\infty d\omega \hbar\omega \hat{\mathbf{f}}^\dagger(\mathbf{r}, \omega) \cdot \hat{\mathbf{f}}(\mathbf{r}, \omega). \quad (1)$$

Here,  $\hat{\mathbf{f}}^\dagger(\mathbf{r}, \omega)$  are bosonic creation operators of effective medium–field excitations.

We apply an external (classical) magnetic field  $\mathbf{B}_{\text{ext}} = B_{\text{ext}}\mathbf{n}$  in order to split the energies of the two neutron spin states. Its directional unit vector  $\mathbf{n}$  is at an angle  $\vartheta$  with respect to the unit normal of the plate. The resulting Hamiltonian of the free neutron reads

$$\hat{H}_N = E_\uparrow |\uparrow\rangle \langle \uparrow| + E_\downarrow |\downarrow\rangle \langle \downarrow|, \quad (2)$$

with energies  $E_{\uparrow/\downarrow} = \pm(\hbar\gamma_n B_{\text{ext}})/2$ . Here,  $\gamma_n$  is the gyromagnetic ratio of the neutron, given by  $\gamma_n = (g_n e)/(2m_n)$

and relates the magnetic dipole moment  $\hat{\mathbf{m}}$  of the neutron to its spin  $\hat{\mathbf{s}}$  via  $\hat{\mathbf{m}} = \gamma_n \hat{\mathbf{s}}$ .  $g_n$  is the  $g$ -factor of the neutron,  $m_n$  its mass and  $e$  the elementary electric charge.

Finally, the interaction Hamiltonian is given by [26]

$$\hat{H}_{\text{int}} = -\hat{\mathbf{m}} \cdot \hat{\mathbf{B}}(\mathbf{r}_N) \quad (3)$$

where  $\hat{\mathbf{B}}$  is the quantised plate-assisted magnetic field

$$\hat{\mathbf{B}}(\mathbf{r}) = \sqrt{\frac{\hbar}{\pi\varepsilon_0}} \int_0^\infty d\omega \frac{\omega}{c^2} \int d^3\mathbf{r}' \sqrt{\text{Im}\varepsilon(\mathbf{r}', \omega)} \times \nabla \times \mathbf{G}(\mathbf{r}, \mathbf{r}', \omega) \cdot \hat{\mathbf{f}}(\mathbf{r}', \omega) + \text{h.c.} \quad (4)$$

Here,  $\mathbf{G}(\mathbf{r}, \mathbf{r}', \omega)$  is the dyadic Green’s tensor for the classical electromagnetic field; it fulfils the integral relation

$$\frac{\omega^2}{c^2} \int d^3s \text{Im} \varepsilon(\mathbf{s}, \omega) \mathbf{G}(\mathbf{r}, \mathbf{s}, \omega) \cdot \mathbf{G}^*(\mathbf{s}, \mathbf{r}', \omega) = \text{Im} \mathbf{G}(\mathbf{r}, \mathbf{r}', \omega). \quad (5)$$

*Casimir–Polder potential.* Starting from an uncoupled state  $|\{0\}\rangle |i\rangle$ , where  $|\{0\}\rangle$  is the vacuum state of the electromagnetic field and  $i \in \{\downarrow, \uparrow\}$ , we use second-order perturbation theory to find its energy shift

$$U_i = \sum_{k=\uparrow, \downarrow} \mathcal{P} \int_0^\infty d\omega \frac{1}{-\hbar(\omega + \omega_{ki})} \int d^3\mathbf{r} \left| \langle i | \langle \{0\} | -\hat{\mathbf{m}} \cdot \hat{\mathbf{B}}(\mathbf{r}_N) | \mathbf{1}(\mathbf{r}, \omega) \rangle | k \rangle \right|^2 \quad (6)$$

where we have defined  $\omega_{ik} = (E_i - E_k)/\hbar$ . We decompose the potential into  $U_i = U_{i\downarrow} + U_{i\uparrow}$ , where the two terms represent the intermediate state being the spin-down and the -up states of the neutron respectively. Using Eqs. (3) and (4) to evaluate the matrix elements of the interaction Hamiltonian, combining the results by means of the integral equation (5) and exploiting Cauchy’s integral formula, one finds

$$U_{\downarrow\downarrow} = U_{\uparrow\uparrow} = \frac{\mu_0}{2} m_{\downarrow\downarrow} \cdot \nabla \times \mathbf{G}^{(1)}(\mathbf{r}_N, \mathbf{r}_N, 0) \times \overleftarrow{\nabla}' \cdot \mathbf{m}_{\downarrow\downarrow}, \quad (7)$$

$$U_{\downarrow\uparrow} = \frac{\mu_0}{\pi} \int_0^\infty d\omega \frac{\omega_{\uparrow\downarrow}}{\xi^2 + \omega_{\uparrow\downarrow}^2} \quad (8)$$

$$\mathbf{m}_{\downarrow\uparrow} \cdot \nabla \times \mathbf{G}^{(1)}(\mathbf{r}_N, \mathbf{r}_N, \omega) \times \overleftarrow{\nabla}' \cdot \mathbf{m}_{\uparrow\downarrow}, \quad (9)$$

$$U_{\uparrow\downarrow} = -U_{\downarrow\uparrow} + \mu_0 \mathbf{m}_{\uparrow\downarrow} \cdot \nabla \times \text{Re}\mathbf{G}^{(1)}(\mathbf{r}_N, \mathbf{r}_N, \omega_{\uparrow\downarrow}) \times \overleftarrow{\nabla}' \cdot \mathbf{m}_{\downarrow\uparrow},$$

where the  $\mathbf{m}_{ij} = \langle i | \hat{\mathbf{m}} | j \rangle$  are the magnetic dipole-matrix elements and  $\mathbf{G}^{(1)}$  is the scattering part of the Green’s tensor. The former can be found by means of rotation operators [27] and are given by

$$\mathbf{m}_{\uparrow\uparrow} = -\mathbf{m}_{\downarrow\downarrow} = \frac{\hbar\gamma_n}{2} (\sin \vartheta, 0, \cos \vartheta), \quad (10)$$

$$\mathbf{m}_{\uparrow\downarrow} = \mathbf{m}_{\downarrow\uparrow}^* = \frac{\hbar\gamma_n}{2} (\cos \vartheta, -i, -\sin \vartheta). \quad (11)$$

*Planar geometry.* In order to calculate the potential further, one has to employ the Green's tensor corresponding to the setup's geometry. In the case of the half space, it reads [26]

$$\mathbf{G}^{(1)}(\mathbf{r}, \mathbf{r}', \omega) = \frac{i}{8\pi^2} \times \int \frac{d^2 \mathbf{k}^\parallel}{k^\perp} \sum_{\sigma=s,p} r_\sigma \mathbf{e}_\sigma \mathbf{e}_\sigma e^{i[\mathbf{k}^\parallel \cdot (\mathbf{r} - \mathbf{r}') + k^\perp(z+z')]}, \quad (12)$$

where  $\mathbf{k}^\parallel$  and  $k^\perp = \sqrt{(w^2)/(c^2) - \mathbf{k}^\parallel{}^2}$  are the components of the wave vector  $\mathbf{k}$  which are parallel and perpendicular to the interface. The incident (-) and reflected (+) plane waves are polarized parallel ( $\sigma = s$ ) or perpendicular ( $\sigma = p$ ) to the interface and are reflected according to the respective Fresnel reflection coefficients  $r_\sigma$ .

*Perfect conductor.* For a perfectly conducting plate with  $r_s = -r_p = -1$ , the potential components (7) and (8) simplify to

$$U_{\downarrow\uparrow} = \frac{\hbar^2 \gamma_n^2 \mu_0}{256 \pi^2 z^3} \int_0^\infty \frac{d\xi \omega_{\uparrow\downarrow}}{\omega_{\uparrow\downarrow}^2 + \xi^2} [f(\frac{\xi z}{c}) + \cos 2\vartheta g(\frac{\xi z}{c})] e^{-2\xi z/c}, \quad (13)$$

$$U_{\downarrow\downarrow} = \frac{\hbar^2 \gamma_n^2 \mu_0}{256 \pi z^3} (1 + \cos^2 \vartheta). \quad (14)$$

with  $f(x) := 5 + 10x + 12x^2$  and  $g(x) := -1 - 2x + 4x^2$ . The mixed potential (13) exhibits two different asymptotes in the retarded,  $(\omega_{\uparrow\downarrow} z)/c \gg 1$ , and the non-retarded regimes,  $(\omega_{\uparrow\downarrow} z)/c \ll 1$ . They read

$$U_{\downarrow\uparrow}^{\text{ret}} = \frac{\hbar^2 \gamma_n^2 \mu_0 c}{32 \pi^2 \omega_{\uparrow\downarrow} z^4}, \quad (15)$$

$$U_{\downarrow\uparrow}^{\text{nr}} = \frac{\hbar^2 \gamma_n^2 \mu_0}{512 \pi} (5 - \cos 2\vartheta) \frac{1}{z^3}. \quad (16)$$

After averaging over the orientation of the external field, the repulsive potential for the ground-state (spin-down) neutron in front of the perfectly conducting plate in the non-retarded regime is given by

$$U_\downarrow = \frac{\hbar^2 \gamma_n^2 \mu_0}{64 \pi} \frac{1}{z^3} \equiv \frac{C_3^N}{z^3}. \quad (17)$$

For comparison, the potential of an atom in front of a perfectly conducting plate ([15]) reads

$$U_A = -\frac{\langle \hat{\mathbf{d}}^2 \rangle}{48 \pi \epsilon_0 z^3} \equiv -\frac{C_3^A}{z^3}, \quad (18)$$

where  $C_3^A = \langle \hat{\mathbf{d}}^2 \rangle / (48 \pi \epsilon_0 z^3)$  is the atomic van der Waals coefficient and  $\hat{\mathbf{d}}$  its electric dipole moment. In an order-of-magnitude estimate, one has  $\langle \hat{\mathbf{d}}^2 \rangle = e^2 a_B^2$ ,  $a_B = (4 \pi \epsilon_0 \hbar^2) / (m_e e^2)$  is the Bohr radius and  $m_e$  is the mass of the electron. Employing  $\gamma = (g_n e) / (2 m_n)$ , with

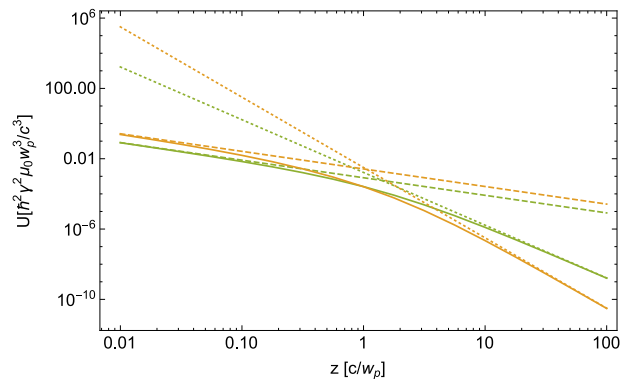


FIG. 2: Constituents of the Casimir-Polder potential of a ground-state (spin-down) neutron in front of a surface described by a plasma model with  $\omega_{\uparrow\downarrow} = \omega_P$ :  $U_{\downarrow\uparrow}$  (yellow) and  $U_{\downarrow\downarrow}$  (green), exact potential (solid), retarded asymptote (dotted) and non-retarded asymptote (dashed).

$g_n = -3.8$  [28] being the  $g$ -factor of the neutron and  $m_n$  being its mass, we find

$$C_3^N = \frac{3}{16} g_n^2 \left( \frac{m_e}{m_n} \right)^2 \alpha^2 C_3^A \approx 1.7 \times 10^{-10} C_3^A, \quad (19)$$

with  $\alpha = e^2 / (4 \pi c \epsilon_0 \hbar) \approx 1/137$  being the fine-structure constant. The Casimir-Polder potential of a neutron in front of a perfectly conducting plate is hence ten orders of magnitude smaller than the corresponding potential of a typical atom, which is due to the smallness of the fine structure constant (accounting for roughly four orders) and the small electron-to-neutron mass ratio (accounting for the remaining six orders).

*Metals and dielectrics.* To be more realistic, we describe the electric response of the plate by the plasma model,  $\epsilon = 1 - \omega_P^2 / \omega^2$ , the Drude model as given by  $\epsilon = 1 - \omega_P^2 / [\omega(\omega + i\gamma\omega)]$  and a single-resonance Drude-Lorentz model,  $\epsilon = 1 - \omega_P^2 / (\omega^2 - \omega_T^2)$ . For each of these models, we find a repulsive ground-state potential. As an illustration, we show its constituents and the respective retarded and non-retarded limits for the plasma model in Fig. 2.

*Discussion.* In an experiment, applied magnetic fields are typically  $B_{\text{ext}} \lesssim 5\text{T}$ , such that the critical distance  $z_{\text{nr}} = c / \omega_{\uparrow\downarrow} = c / (\gamma_n B_{\text{ext}}) \gtrsim 0.32\text{m}$  for the non-retarded limit is much larger than typical distances in experiments which vary from nm to  $\mu\text{m}$ . We have  $z \ll z_{\text{nr}}$ , such that we find ourselves in the non-retarded limit. For all practical cases, we can hence expand the potential to leading order of the external magnetic field. The results are summarised in Tab. I. For the perfect conductor and the plasma model, the potential persists even of vanishing external magnetic field. For the two other models instead, the potential is linear in the applied magnetic field.

We note that the different models lead to a variety of asymptotic power laws for the distance dependence. For

Model	$U_{\downarrow}$
Perf. cond.	$\frac{\hbar^2 \gamma_n^2 \mu_0}{64\pi z^3}$
Plasma	$\frac{\hbar^2 \gamma_n^2 \mu_0 \omega_p^2}{128\pi c^2 z}$
Drude	$-\frac{\hbar^2 \gamma_n^2 \mu_0 \omega_p^2 (2 + \sin^2 \vartheta)}{256\pi^2 c^2 z} \frac{\gamma_n B_{\text{ext}}}{\gamma} \ln \frac{\gamma_n B_{\text{ext}}}{\gamma}$
Drude-Lorentz	$\frac{\hbar^2 \gamma_n^2 \mu_0 \omega_p^2}{192\pi c^2} \frac{\omega_T + \omega_L}{\omega_T \omega_L} \frac{1}{z} \gamma_n B_{\text{ext}}$

TABLE I: Non-retarded ground-state potential  $U_{\downarrow}$  for different models within leading order in the applied magnetic field.  $\omega_L = \sqrt{\omega_T^2 + \omega_p^2}/2$

instance, it is seen that the perfect-conductor limit does not commute with the nonretarded limit for the plasma model, in contrast to the case of the atomic Casimir-Polder potential [29]. In addition, there are marked differences between the plasma and Drude models, making this interaction a new and sensitive test case for the Drude-plasma debate in Casimir physics [30, 31]. Ultimately, the strong model-dependence of the neutron Casimir-Polder potential stems from its mixed electric-magnetic interaction in a short-distance regime, which is analogous to the case of the anomalous magnetic moment of the electron [32].

Finally, let us discuss whether the potentials predicted for the different models are in principle detectable in an experiment. To that end, we compare them with the gravitational potential exerted on the neutron by the same plate and by earth, respectively. In Fig. 3 the neutron Casimir-Polder potential at accessible distance regimes is shown for the different models alongside these two gravitational potentials. To estimate the gravitational field of the surface, we have for simplicity used a silicon sphere (density  $\rho = 2.33 \text{ g/cm}^3$ ) of radius  $r = 11.3 \text{ mm}$  whose mass is comparable to that of a plate in a typical neutron interferometry experiment [25]. The magnitude of the Casimir-Polder potential is highly model-dependent. While it is generally weaker than the gravitational potential of earth (except for the perfect-conductor case), it is for all models stronger than the gravitational potential of the plate itself. It should hence be taken into account when performing short-range gravity experiments with neutrons.

*Conclusions.* We have shown that a single neutron under the influence of a constant magnetic field will be subject to a Casimir-Polder-type dispersion interaction with a metal or dielectric plate. This is an example of Casimir repulsion for a magnetisable object interacting with a polarisable one where the repulsion is not dominated by an electric-electric force. We have found that the force is non-retarded for experimentally accessible regimes and that it is very sensitive to the electric re-

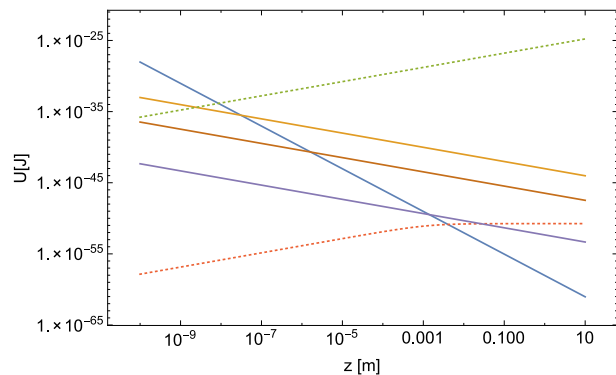


FIG. 3: Ground-state Casimir-Polder potential of a neutron in front of a surface with applied field  $B_{\text{ext}} = 2 \text{ T}$  (solid lines) compared to gravitational potentials (dashed): Perfect conductor (blue), plasma model for gold (yellow,  $\omega_p = 1.37 \times 10^{16} \text{ rad/s}$  [33]), Drude model for gold (red,  $\gamma = 4.10 \times 10^{12} \text{ rad/s}$  [33]), Drude-Lorentz model for silicon (purple,  $\omega_p = 2.3 \times 10^{16} \text{ rad/s}$ ,  $\omega_T = 7.1 \times 10^{16} \text{ rad/s}$  [34]), gravitational potentials of earth (green) and of silicon sphere (red).

sponse of the surface. It may hence provide a testing ground for the Drude-plasma debate. In addition, it can become comparable to the gravitational interaction of the same surface and is hence relevant to the probing for non-standard gravity on small scales.

*Acknowledgements.* We are grateful for discussions with H. Rauch, H. Lemmel and H. Fichter. This work was supported by the German Research Foundation (DFG, grants BU 1803/3-1 and GRK 2079/1) and the Freiburg Institute for Advanced Studies.

- 
- [1] H. B. G. Casimir, Proc. K. Ned. Akad. Wet. **51**, 793 (1948).
  - [2] E. M. Lifshitz, Sov. Phys. JETP **2**, 73 (1956).
  - [3] P. W. Milonni, *The Quantum Vacuum* (Academic Press, New York, 1994).
  - [4] H. B. G. Casimir and D. Polder, Phys. Rev. **73**, 360 (1948).
  - [5] T. H. Boyer, Phys. Rev. A **9**, 2078 (1974).
  - [6] V. Hushwater, Am. J. Phys. **65**, 381 (1997).
  - [7] G. Feinberg and J. Sucher, J. Chem. Phys. **48**, 3333 (1968).
  - [8] A. Salam, Int. J. Quantum Chem. **78**, 437 (2000).
  - [9] O. Kenneth, I. Klich, A. Mann and M. Revzen, Phys. Rev. Lett. **89**, 033001 (2002).
  - [10] C. Henkel and K. Joulain, Europhys. Lett. **72**, 929 (2005).
  - [11] T. H. Boyer, Phys. Rev. **180**, 19 (1969).
  - [12] Y. Tikochinsky and L. Spruch, Phys. Rev. A **48**, 4236 (1993).
  - [13] S. Y. Buhmann, D.-G. Welsch and T. Kampf, Phys. Rev. A **72**, 032112 (2005).
  - [14] H. Safari, D.-G. Welsch, S. Y. Buhmann and S. Scheel, Phys. Rev. A **78**, 062901 (2008).

- [15] J. E. Lennard-Jones, *Trans. Faraday Soc.* **28**, 333 (1932).
- [16] C. Farina, F. C. Santos and A. C. Tort, *J. Phys. A: Math. Gen.* **35**, 2477 (2002).
- [17] C. Farina, F. C. Santos and A. C. Tort, *Am. J. Phys.* **70**, 421 (2002).
- [18] F. M. Serry, D. Walliser and G. J. Maclay, *J. Appl. Phys.* **84**, 2501 (1998).
- [19] J. N. Munday, F. Capasso and V. A. Parsegian, *Nature* **457**, 170 (2009).
- [20] J. M. Obrecht, R. J. Wild, M. Antezza, L. P. Pitaevskii, S. Stringari and E. A. Cornell, *Phys. Rev. Lett.* **98**, 063201 (2007).
- [21] H. Failache, S. Saitiel, M. Fichet, D. Bloch, M. Ducloy, *Phys. Rev. Lett.* **83**, 5467 (1999).
- [22] F. S. S. Rosa, D. A. R. Dalvit and P. Milonni, *Phys. Rev. Lett.* **100**, 183602 (2008).
- [23] F. S. S. Rosa, D. A. R. Dalvit and P. Milonni, *Phys. Rev. A* **78**, 032117 (2008).
- [24] S. J. Rahi, M. Kardar and T. Emig, *Phys. Rev. Lett.* **105**, 070404 (2010).
- [25] H. Rauch, H. Lemmel, M. Baron and R. Loidl, *Nature* **417**, 630 (2002).
- [26] S. Y. Buhmann, *Dispersion Forces I—Macroscopic Quantum Electrodynamics and Ground-State Casimir, Casimir–Polder and van der Waals Forces* (Springer, Heidelberg, 2012).
- [27] J. J. Sakurai, *Modern Quantum Mechanics* (Addison–Wesley, New York, 1994).
- [28] H. Stöcker, *Taschenbuch der Physik*, 2nd Ed. (Harri Deutsch, Frankfurt, 1994).
- [29] M. Babiker and G. Barton, *J. Phys. A: Math. Gen.* **9**, 129 (1976).
- [30] I. Brevik, S. A. Ellingsen, K. A. Milton, *New J. Phys.* **8**, 236 (2006).
- [31] M. Bordag, G. L. Klimchitskaya, U. Mohideen, V. M. Mostepanenko, *Advances in the Casimir effect* (Oxford University Press, Oxford, 2009) and references therein.
- [32] R. Bennett and C. Eberlein, *Phys. Rev. A* **88**, 012107 (2013).
- [33] Palik, E. D. (ed.), *Handbook of Optical Constants of Solids III* (Academic Press, New York, 1991).
- [34] I. Pirozhenko and A. Lambrecht, *Phys. Rev. A* **77**, 013811 (2008).